Supporting Information for

Site dependent reactivity of Pt single atoms on anatase TiO$_2$ (101) in aqueous environment

Bo Wen[a, b], Wen-Jin Yin[d], Annabella Selloni*[b], Li-Min Liu*[c, a]

(a) Beijing Computational Science Research Center, Beijing 100193, China

(b) Department of Chemistry, Princeton University, Princeton, New Jersey 08544, United States

(c) School of Physics, Beihang University, Beijing 100191, China

(d) School of Physics and Electronic Science, Hunan University of Science and Technology, Xiangtan 411201, China

I- Assessing the performance of PBE+U$_d$+U$_p$

(a) Bulk properties

To assess the performance of PBE+U$_d$+U$_p$, we compared the structural and electronic properties of bulk anatase obtained with this method to those given by pure PBE and PBE+U$_d$ (U$_d$=U$_p$=3.5 eV). Due to the unavailability of band structure in CP2K, the calculations were conducted using the Quantum Espresso package.[1] However, our calculations of DOS are similar by both software packages. As shown by **Table S1**, PBE predicts the best lattice parameters and the worst band gap in comparison to experiment. PBE+U$_d$ worsens the description of the structure while improving the band gap by only 0.2 eV. In contrast, PBE+U$_d$+U$_p$ maintains a reasonable description of the geometry while improving the electronic structure quite remarkably. The densities of states and band structures computed with the three methods are reported in **Figure S1**. We can see that PBE+U$_d$ leads to a contraction of the CB by nearly 1 eV in comparison to pure PBE. PBE+U$_d$+U$_p$

induces a similar contraction, but also an upward shift of the CBM by nearly 1 eV and an expansion of the VB by about 0.5 eV compared with PBE and PBE+U_d. As a result, the PBE+U_d+U_p band gap is very close to the experimental value.

Table S1 Comparison of anatase lattice parameters and band gaps calculated by different methods.

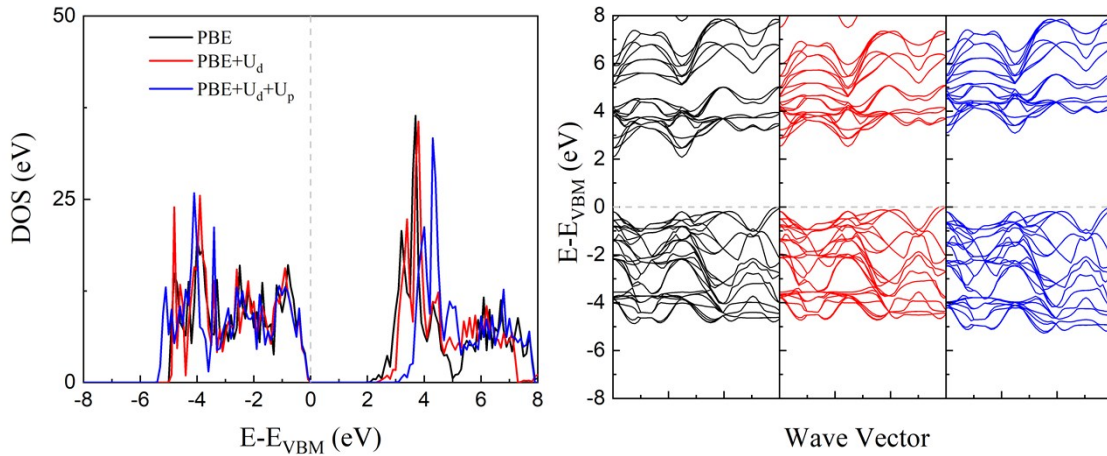| Functional	a/c (Å)	error	Band gap (eV)
PBE	3.796	0.3%	2.2
	9.680	1.7%	
PBE+U_d	3.824	1.0%	2.4
	9.743	2.4%	
PBE+U_d+U_p	3.797	0.3%	3.1
	9.769	2.7%	
Experiment	3.785		3.2
	9.514		

Figure S1 Electronic density of states (DOS) and band structure of bulk anatase calculated by different methods. The dashed grey lines indicate the VBM, which take as the zero of energy.

(b) Relative stabilities of different Pt adsorption structures

To further assess the performance of PBE+U_d+U_p, we compared the results obtained using PBE, PBE+U_d and PBE+U_d+U_p for the three lowest energy Pt adsorption configurations reported in Ref.[2]. As shown in **Figure S2,** both PBE and PBE+U_d+U_p predict configuration (site) 3 to be most stable, whereas site 2 is more stable than 3 according to PBE+U_d. However, whereas PBE and PBE +U_d predict a very small energy difference between site 2 and 3, the difference is much larger, 0.44 eV, with PBE+U_d+U_p. Site 3 is significantly more stable than any other site using PBE+U_d+U_p and is thus taken as the stable configuration of a Pt adatom on the stochiometric surface in our work.
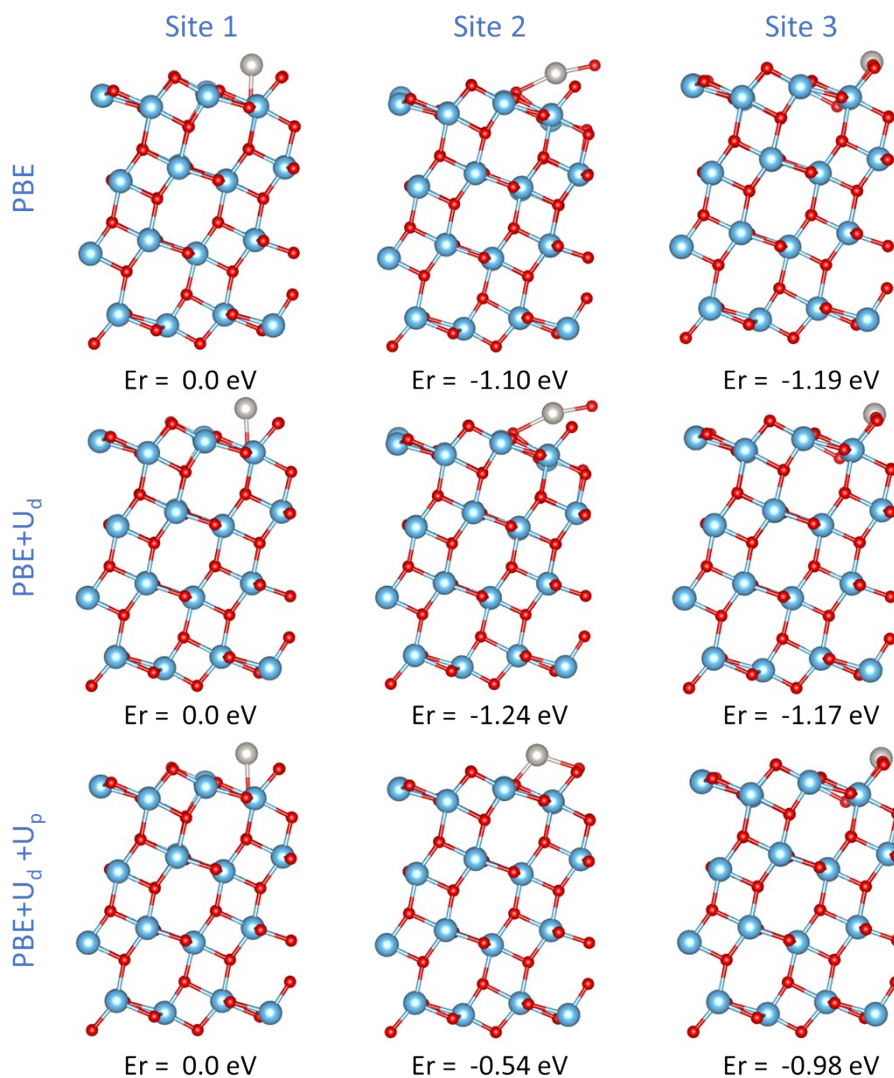
Figure S2 Computed Pt adsorption structures and energies on stoichiometric anatase (101) as obtained using PBE, PBE+U_d and PBE+U_d+U_p. With each method, the reference energy is that of site 1.

II- Charge analysis

Two different methods, DDEC6 and Mulliken charge,[3-5] have been used to estimate the charge on the Pt atom in the different investigated models. Neither method is quantitatively accurate, but trends are expected to be reliable. Both methods predict Pt_O and Pt_{Ti} to be negatively and positively charged, respectively, while the charge on Pt_S is very small. The reduced Pt_{Ti} and PtOH are also positively charged but become less and less than Pt_{Ti}. This trend of charge transfer has also been found in a recent study.[6]

Table S2 DDEC6 and Mulliken charges[3-5] for the various systems examined in this work, calculated at the PBE+U_d+U_p level. In some cases, PBE results are also reported (in red). For A-Pt_O and A-Pt_{Ti}, the charge in the presence of dissociated water is also evaluated.

Method	Geometry		Pt	Ti	O of TiO_2	O of dH_2O	H of dH_2O
DDEC Analysis	A-Pt_S	no H_2O	-0.14	2.40 – 2.56	-1.32 – -0.95		
	A-Pt_O	no H_2O	-0.65	2.17 – 2.57	-1.32 – -1.08		
		with H_2O	-0.31	2.21 – 2.57	-1.33 – -1.07	-0.98	-0.05/0.47
	A-Pt_{Ti}	no H_2O	1.67	2.45 – 2.57	-1.32 – -1.08		
		with H_2O	1.73	2.45 – 2.57	-1.32 – -1.08	-0.81	0.41/0.49
Mulliken Analysis	A-Pt_S	no H_2O	-0.05 0.03	1.51 – 1.61 1.09 – 1.18	-0.89 – -0.66 -0.67 – -0.47		
	A-Pt_O	no H_2O	-0.37 -0.24	1.57 – 1.61 1.06 – 1.18	-0.89 – -0.66 -0.67 – -0.47		
		with H_2O	-0.31 -0.24	1.46 – 1.61 1.05 – 1.18	-0.89 – -0.66 -0.68 – -0.47	-0.52 -0.35	0.15/0.19 0.15/0.16
	A-Pt_{Ti}	no H_2O	0.86 0.78	1.58 – 1.64 1.14 – 1.18	-0.89 – -0.66 -0.69 – -0.40		
		with H_2O	0.78 0.72	1.58 – 1.66 1.14 – 1.22	-0.89 – -0.56 -0.68 – -0.40	-0.48 -0.33	0.19/0.22 0.14/0.18
	A-Pt_{Ti}+O_v	no H_2O	0.44	1.57 – 1.63	-0.89 – -0.57		
	A-PtOH	no H_2O	0.32	1.58 – 1.61	-0.89 – -0.66		
	A-PtO_2	no H_2O	0.82	1.58 – 1.61	-0.89 – -0.65		

III- Effect of Pt on oxygen vacancy formation and distribution

Table S3 Formation energy (in eV) of surface and subsurface oxygen vacancies on clean and Pt-loaded anatase (101) computed using the PBE+U_d+U_p method. In the presence of Pt, the formation energy is given for both an O_v in proximity of the Pt atom and away from it (between parentheses).

The formation energy is computed as:
$$E_f = E_{slab + O_v} - (E_{slab} - \frac{1}{2} \cdot E_{O^2})$$

System	Surface O_v	Subsurface O_v
Clean surface	3.80	3.77
A-Pt$_S$	1.78 (3.56)	3.13 (3.51)
A-Pt$_O$	3.64 (3.97)	4.06 (3.52)
A-Pt$_{Ti}$	1.25 (2.71)	0.54 (2.92)

a

A-Ov-Pt1
E_r=0.00 eV

A-Ov-Pt2
E_r=0.25 eV

A-Ov-Pt3
E_r=-0.19 eV

A-Ov-Pt4
E_r=0.40 eV

A-Ov-Pt5
E_r=-0.63 eV

A-Ov-Pt6
E_r=0.12 eV

A-Ov-Pt7
E_r=-0.34 eV

b

A-Ovs-Pt1
E_r=-1.91 eV

A-Ovs-Pt2
E_r=0.96 eV

A-Ovs-Pt3
E_r=0.44 eV

A-Ovs-Pt4
E_r=0.23 eV
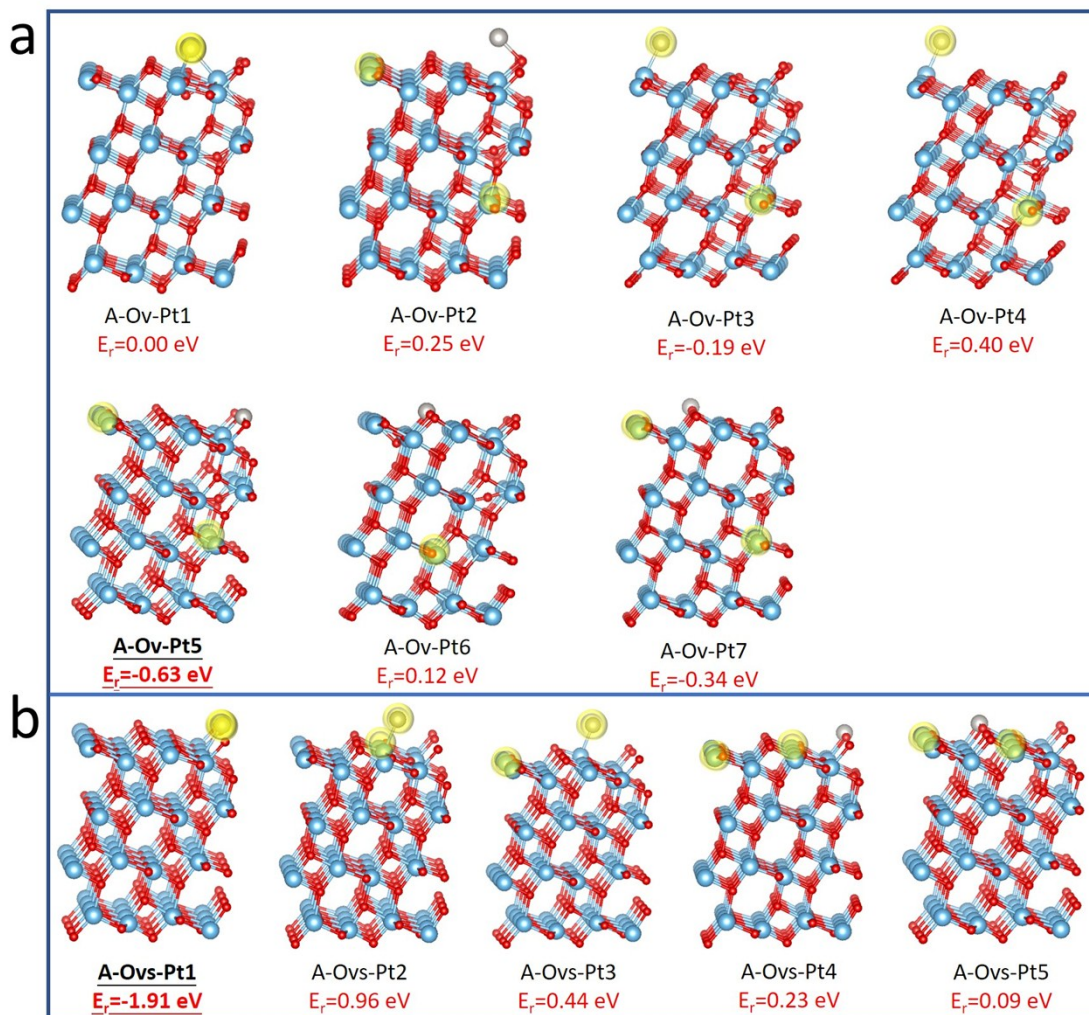
A-Ovs-Pt5
E_r=0.09 eV

Figure S3 Adsorption configurations of a Pt atom on reduced anatase (101) with: (a) subsurface O_v or (b) surface O_v. The energy for each structure relative to A-O_v-Pt1 is given. Bold characters are used for the most stable configuration of each case. Circles shaded in yellow indicate the locations of the excess electrons.
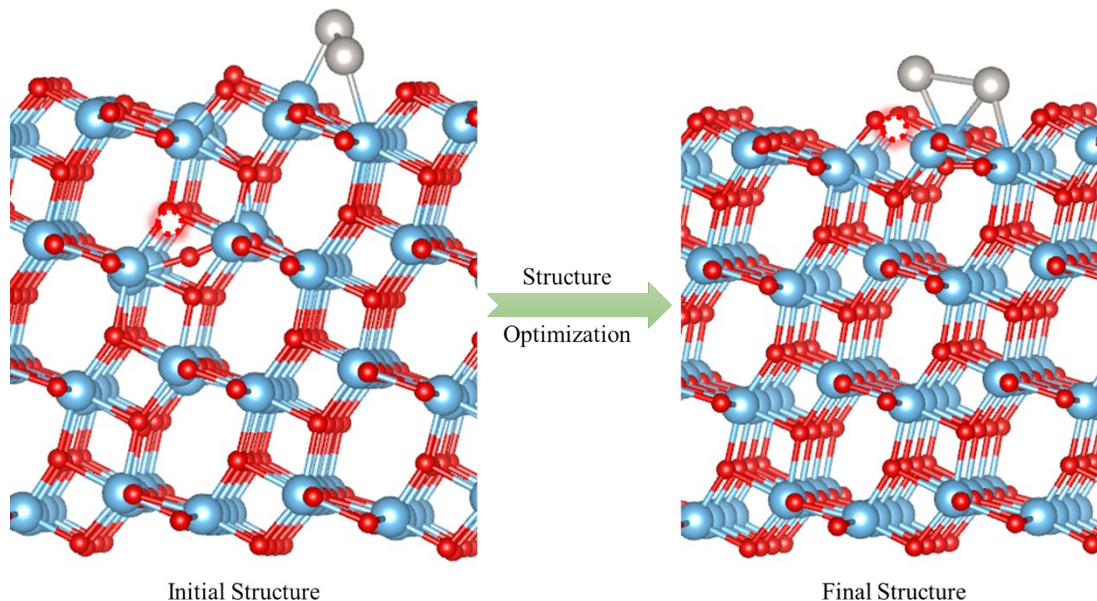

Initial Structure   Final Structure

Figure S4 Structural optimization of an anatase (101) slab with a subsurface O_v and two Pt adatoms (left panel) leads to spontaneous diffusion of the O_v to the surface (right). White stars with red halos highlight the position of the O_v.
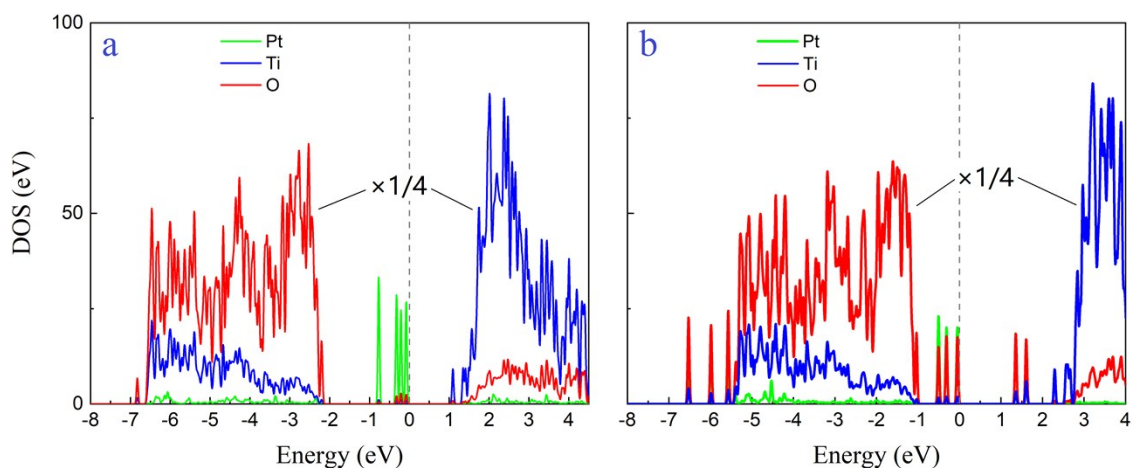

Figure S5 Electronic density of states for: (a) A-Pt_{Ti} with a close O_v, and (b) A-PtO_2 on the stochiometric surface. The Fermi energy (E_F) is set at the HOMO and is taken as the zero of energy. For better visualization, the partial DOS of Ti and O atoms are rescaled by a factor of 0.25.

6

IV- Effect of Pt on water adsorption and aqueous TiO_2 interfaces

The adsorption energies of an intact and a dissociated water molecule on the three of the surfaces shown in **Figure 1** are reported in **Table S4** while a few structures and corresponding DOS are presented in **Figure S6.** While molecular adsorption is always more or at most equally favorable in comparison to the dissociated state, in both the PBE+U_d+U_p and PBE calculations the presence of Pt generally reduces the energy difference between the molecular and dissociated state. Note that in the case of molecular adsorption the water molecule is always adsorbed on a fivefold Ti site near the Pt except in the case of Pt_{Ti}, where it is adsorbed directly on the Pt replacing a Ti atom.

Table S4 Adsorption energy (E_a) of an intact and dissociated water molecule on different surfaces, from PBE and PBE+U_d+U_p calculations. E_a is computed as: $E_a = E_{slab + H_2O} - (E_{slab} + E_{H_2O})$. (unit: eV). The PBE results for clean anatase are in good agreement with previous studies[7]

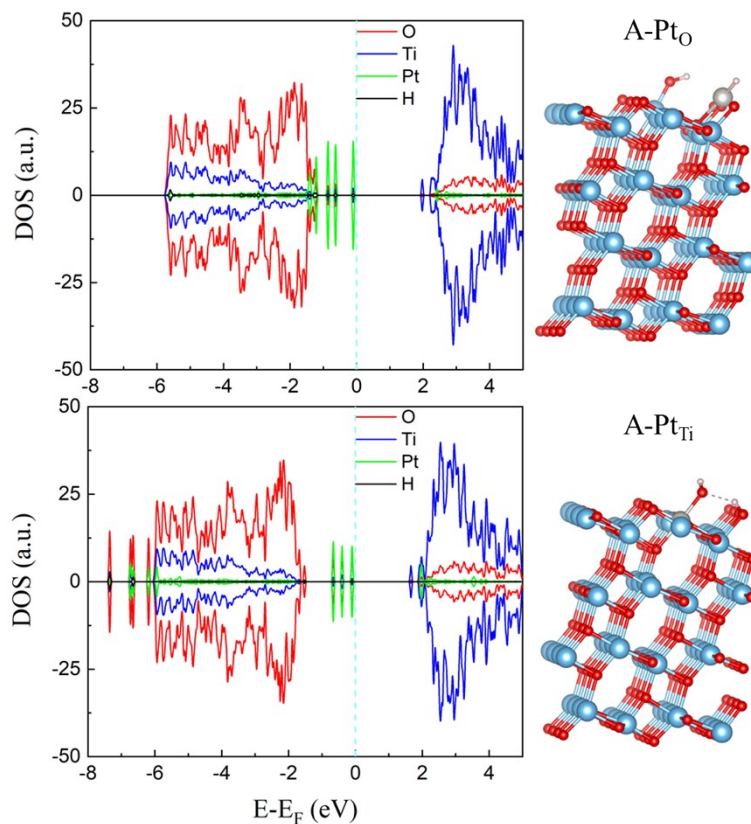| Surface	E_a-intact (PBE)	E_a-disso (PBE)	E_a-intact (PBE+U_d+U_p)	E_a-disso (PBE+U_d+U_p)
Clean	-0.71	-0.32	-0.64	-0.48
A-Pt_S	-0.76	-0.63	-0.75	-0.74
A-Pt_O	-0.74	-0.62	-0.65	-0.42
A-Pt_{Ti}	-1.32	-0.94	-1.36	-1.36

Figure S6 Atomic structure and electronic density of states of the A-Pt$_O$ and A-Pt$_{Ti}$ surfaces with an adsorbed water in dissociated form. The Fermi energy (E$_F$) is set at the HOMO and is taken as the zero of energy. The partial DOS of Ti and O atoms are rescaled by a factor of 0.25. Red, blue, green and black lines in DOS plot are partial DOS of O, Ti, Pt and H, respectively.
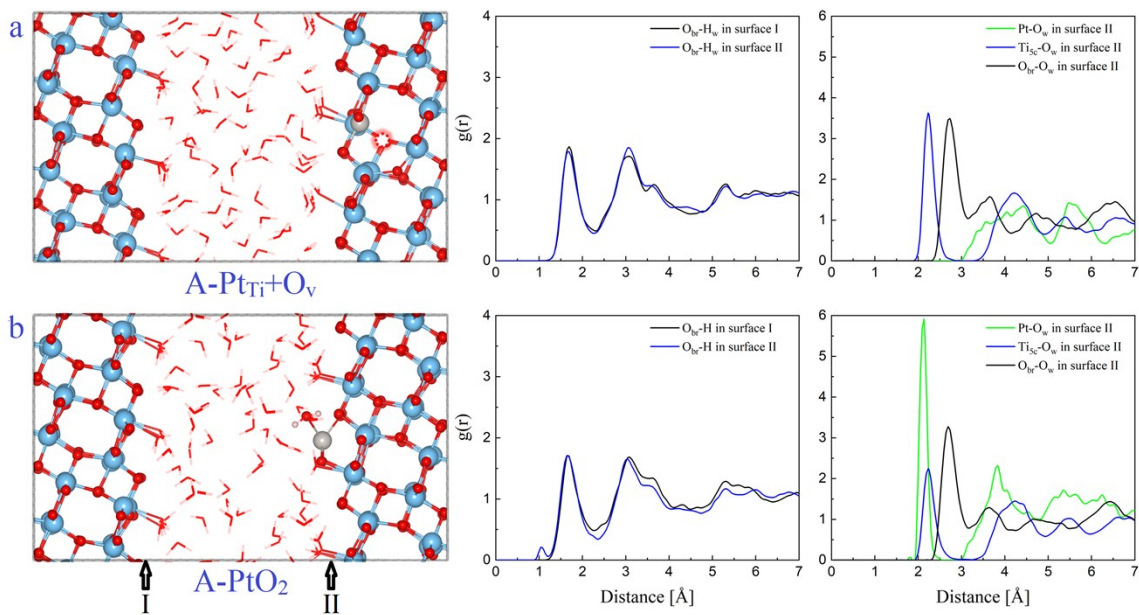
Figure S7 Snapshots from PBE-based BOMD simulations (left) and O_{br}-H_w (middle) and surface II-water (including Pt_{Ti}-O_w, Ti_{5c}-O_w and O_{br}-O_w) pair distribution functions (right) for the aqueous interfaces of: (a) A-Pt_{Ti} + O_v, and (b) A-PtO_2. Blue, red, grey, and white spheres (sticks) represent Ti, O, Pt and H atoms, white stars with red halos represent O_v.
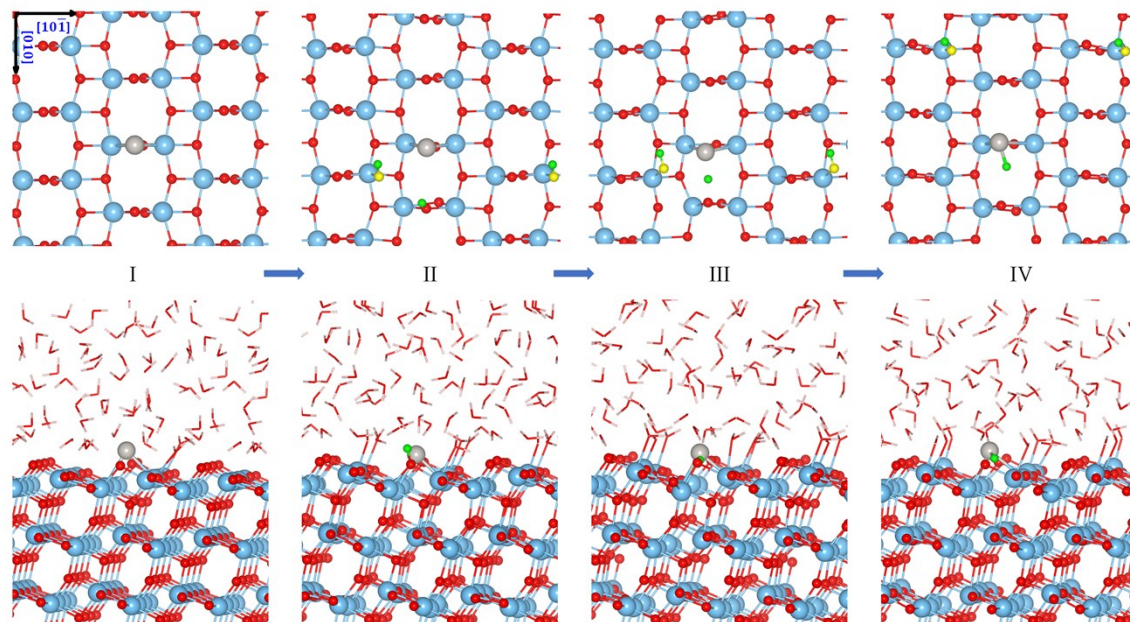

Figure S8 Water dissociation and proton diffusion at the water-A-Pt_O interface. For better visualization, both side (bottom) and top views (top) are presented. In the latter, only the anatase surface and the dissociated water molecule (Oxygen in yellow, H in green) are shown; the apparent presence of two OH groups is an effect of the periodic boundary conditions.
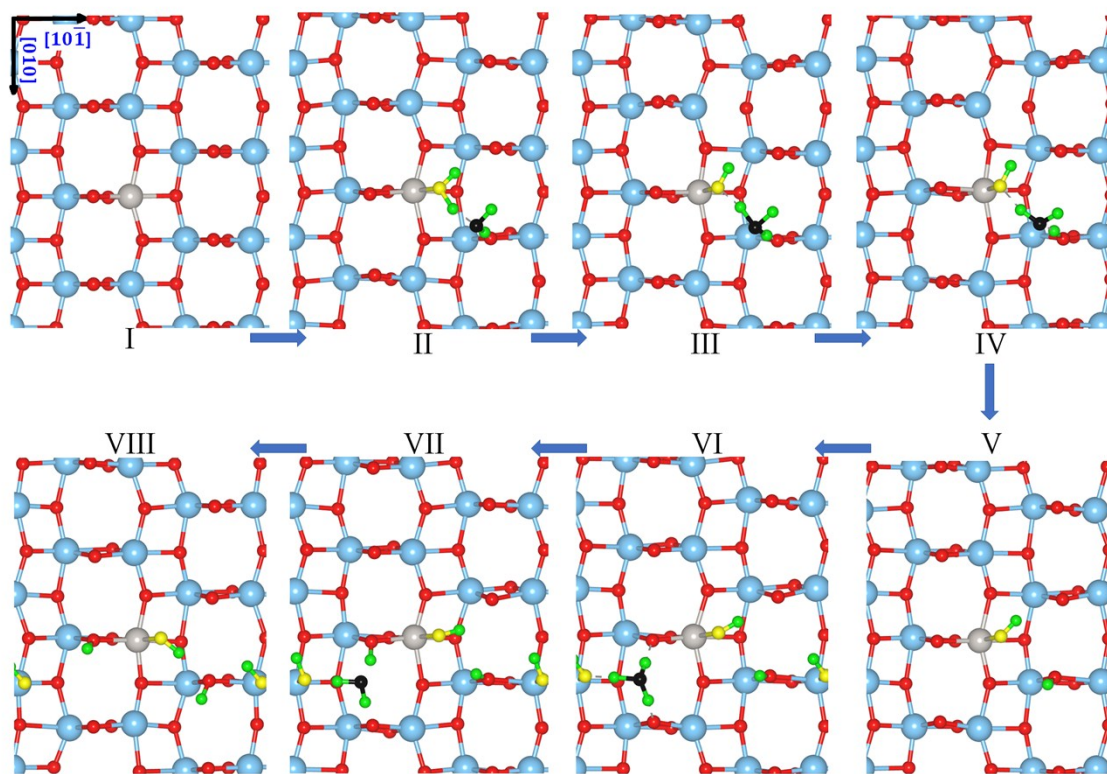
Figure S9 Water dissociation and proton diffusion at the water-A-Pt$_{Ti}$ interface. For better visualization, only the anatase surface and the relevant water molecules are shown. Yellow and black spheres represent O from water in first and second layer, respectively; H atoms are shown in green. Two water dissociation events are shown, both mediated by a second layer water molecule.

References:

1 P. Giannozzi, S. Baroni, N. Bonini, M. Calandra, R. Car, C. Cavazzoni, D. Ceresoli, G. L. Chiarotti, M. Cococcioni, I. Dabo, A. Dal Corso, S. de Gironcoli, S. Fabris, G. Fratesi, R. Gebauer, U. Gerstmann, C. Gougoussis, A. Kokalj, M. Lazzeri, L. Martin-Samos, N. Marzari, F. Mauri, R. Mazzarello, S. Paolini, A. Pasquarello, L. Paulatto, C. Sbraccia, S. Scandolo, G. Sclauzero, A. P. Seitsonen, A. Smogunov, P. Umari and R. M. Wentzcovitch, *J. Phys. Condens. Matter*, 2009, **21**, 395502.
2 H. Wang, T. An and A. Selloni, *J. Chem. Phys.*, 2017, **146**, 184703.
3 N. G. Limas and T. A. Manz, *RSC Advances*, 2016, **6**, 45727-45747.
4 T. A. Manz and N. G. Limas, *RSC Advances*, 2016, **6**, 47771-47801.
5 R. S. Mulliken, 1955, **23**, 1833-1840.
6 H. V. Thang, G. Pacchioni, L. DeRita and P. Christopher, *J. Catal.*, 2018, **367**, 104-114.
7 C. Sun, L.-M. Liu, A. Selloni, G. Q. Lu and S. C. Smith, *J. Mater. Chem.*, 2010, **20**, 10319-10334.